Dipolar bright solitons and solitary vortices in a radial lattice

Chunqing Huang, Lin Lyu, Hao Huang, Zhaopin Chen, Shenhe Fu, Haishu Tan, Boris A. Malomed, and Yongyao Li

Phys. Rev. A **96**, 053617 — Published 13 November 2017

DOI: 10.1103/PhysRevA.96.053617

Dipolar bright solitons and solitary vortices in a radial lattice

Chunqing Huang[1], Lin Lyu[1], Hao Huang[1], Zhaopin Chen[2],
Shenhe Fu[3], Haishu Tan[1], Boris A. Malomed[2,4,1], and Yongyao Li[1,5*]
[1] *School of Physics and Optoelectronic Engineering, Foshan University, Foshan 528000, China*
[2] *Department of Physical Electronics, School of Electrical Engineering, Faculty of Engineering, and the Center for Light-Matter Interaction, Tel Aviv University, Tel Aviv 69978, Israel*
[3] *Department of Optoelectronic Engineering, Jinan University, Guangzhou 510632, China*
[4] *Laboratory of Nonlinear-Optical Informatics, ITMO University, St. Petersburg 197101, Russia*
[5] *College of Electronic Engineering, South China Agricultural University, Guangzhou 510642, China*

Stabilizing vortex solitons with high values of the topological charge, S, is a challenging issue in optics, studies of Bose-Einstein condensates (BECs) and other fields. To develop a new approach to the solution of this problem, we consider a two-dimensional dipolar BEC under the action of an axisymmetric radially periodic lattice potential, $V(r) \sim \cos(2r + \delta)$, with dipole moments polarized perpendicular to the system's plane, which gives rise to isotropic repulsive dipole-dipole interactions (DDIs). Two radial lattices are considered, with $\delta = 0$ and π, i.e., a potential maximum or minimum at $r = 0$, respectively. Families of vortex gap soliton (GSs) with $S = 1$ and $S \geq 2$, the latter ones often being unstable in other settings, are completely stable in the present system (at least, up to $S = 11$), being trapped in different annular troughs of the radial potential. The vortex solitons with different S may stably coexist in sufficiently far separated troughs. Fundamental GSs, with $S = 0$, are found too. In the case of $\delta = 0$, the fundamental solitons are ring-shaped modes, with a local minimum at $r = 0$.At $\delta = \pi$, they place a density peak at the center.

PACS numbers: 42.65.Tg; 03.75.Lm; 47.20.Ky; 05.45.Yv

I. INTRODUCTION

Nonlinear optical and matter waves carrying angular momentum readily self-trap into vortex modes, which may be considered as two-dimensional dark solitons supported by a modulationally stable flat background, or bright solitons with embedded vortices. Experimental and theoretical studies of vortices is a vast research area in nonlinear optics, studies of Bose-Einstein condensates (BECs), quantum fluids, and in other fields. The formation, stability, and dynamics of dark [1–13] and bright [14–49] vortices have been explored in a great variety of settings, including conservative and dissipative ones, continuous and discrete media, local and nonlocal interactions, and different types of the nonlinearity – cubic (self-focusing and defocusing), cubic-quintic, saturable, and quadratic (second-harmonic generating). A recent development has produced unexpected predictions in the form of bright semi-vortices (bound states of components with vorticities $S = 0$ and $S = 1$) in spinor BECs with the spin-orbit coupling and contact attractive interactions, which are stable in free space [50–55],as well as stable gap solitons of the semi-vortex type in the free space with dipole-dipole interactions (DDIs) [56].

In many cases, bright vortex solitons are stable solely with the unitary topological charge, $S = 1$. In particular, the spin-orbit coupling supports solitons with vorticities $S = 1$ and $S = 2$ in its two components, which are completely unstable [50, 56]. Vortices in the self-attractive BEC trapped in an harmonic-oscillator potential also have a stability area solely for $S = 1$ [14, 19, 32, 34]. Vortex solitons in the free space with the cubic-quintic nonlinearity [15] feature stability regions for $S > 1$, but they are very narrow, starting from $S = 3$ [17]. Typically, the vortex solitons with $S > 1$ are subject to azimuthal perturbations which break them into S fragments [19, 34, 57, 58]. This instability has been demonstrated experimentally for vortex beams propagating in saturable self-focusing media [59–61], as well as in quadratic ones [62].

Sufficiently large stability regions in the parametric space for vortex solitons with $S > 1$ were found in axisymmetric potential lattices with the Bessel functional profile in the radial direction, combined with the self-defocusing nonlinearity [63]. In that case, a deeper lattice is required to stabilize solitary vortices with higher values of S. Because the Bessel potential vanishes at $r \to \infty$, the total norm of modes trapped in it under the action of self-defocusing, strictly speaking, diverges in the infinite space. Truly confined gap solitons (GSs), i.e., solitons whose chemical potential falls in one of bandgaps generated by the underlying potential lattice, were constructed considering the combination of the self-defocusing cubic nonlinearity and a radially-periodic potential, $\sim \cos(2kr)$, where r is the radial coordinate [64]. However, only radial GSs with $S = 0$ were found to be completely stable in the latter model, while all confined vortices featured a weak azimuthal instability. Self-trapped vortices, which remain stable, at least, up to $S = 5$, were recently found in a model of a polariton type, which combines the self-repulsive contact nonlinearity of a two-component BEC and effective nonlocal

*Electronic address: yongyaoli@gmail.com

self-attraction mediated by the microwave field generated by transitions between two components resonantly coupled by the field [48]. Nonlocal interactions, considered in Ref. [48], or in the present work (see below), introducing their own radial scale, provide more options in the interplay with the radially-periodic lattice, which helps, in particular, to stabilize vortex GS modes against the azimuthal instability.

The objective of the present work is to predict stable GSs with $S = 0$ and $S \geq 1$ in a dipolar BECs trapped in a radially periodic potential, with dipole moments polarized perpendicular to the system's plane, which gives rise to the isotropic repulsive DDI. In earlier works, DDIs were used to predict stable one-dimensional [65–68] and two-dimensional [69–79] solitons in other settings. In addition, it was found that quadrupole-quadrupole interactions are also able to create stable two-dimensional solitons [80, 81].However, the free-space DDI per se cannot stabilize vortex solitons with $S > 1$ [71]. In this work, we demonstrate that ring-shaped vortex GSs with higher values of S (at least, up to $S = 11$) are readily made stable by the combined effect of the radial lattice potential and repulsive isotropic DDIs. Furthermore, double and multiple sets of concentric vortex solitons, with different topological charges, may stably coexist, if placed in different annular potential troughs of the radial lattice. In that case, vorticity jumps take place at zero-amplitude notches separating the concentric vortices. The latter property was not reported in previously considered two-dimensional models.

The paper is structured as follows. The model is introduced in Sec. II, which is followed by presentation of numerical results for the fundamental ($S = 0$) and vortex ($S \geq 1$) GSs in Sec. III. The stability of the solitons is verified by means of systematic direct simulations. The paper is concluded by Sec. IV.

II. THE MODEL

According to what is said above, we consider an effectively two-dimensional setting, modeled by Gross-Pitaevskii equation, which is written in the scaled form:

$$i\frac{\partial}{\partial t}\Psi(\mathbf{r},t) = -\frac{1}{2}\nabla^2\Psi(\mathbf{r},t) + V(r)\Psi(\mathbf{r},t) + \kappa\Psi(\mathbf{r},t)\int R(\mathbf{r}-\mathbf{r}')|\Psi(\mathbf{r}',t)|^2 d\mathbf{r}', \tag{1}$$

where $\mathbf{r} = \{x, y\}$ is the set of coordinates, $\nabla^2 = \partial_x^2 + \partial_y^2$ is the respective Laplacian, $\Psi(\mathbf{r}, t)$ is the mean-field wave function, and $\kappa > 0$ is the strength of the DDI, with the isotropic kernel corresponding to the particles' dipolar moments polarized perpendicular to the (x, y) plane:

$$R(\mathbf{r}-\mathbf{r}') = \frac{1}{[\epsilon^2 + (\mathbf{r}-\mathbf{r}')^2]^{3/2}}. \tag{2}$$

Here, cutoff ϵ is the regularization parameter, which is determined by the confinement of the three-dimensional condensate in the transverse direction [65, 66]. Further, the axisymmetric radially-periodic lattice potential is taken as

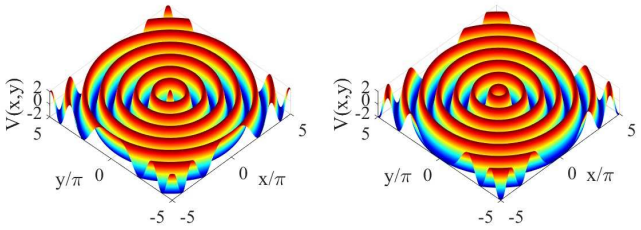

FIG. 1: Radial potentials (3) with $V_0 = 1$, for $\delta = 0$ (a) and $\delta = \pi$ (b).

$$V(r) = V_0 \cos(2r + \delta), \tag{3}$$

where $r = \sqrt{x^2 + y^2}$, the depth of the lattice potential is $2V_0 > 0$, the radial period is fixed to be π by scaling, and δ is a phase constant. Here, we focus on the consideration of two most essential cases, *viz.*, $\delta = 0$ and $\delta = \pi$, which correspond to a potential maximum or minimum at the center, $r = 0$, respectively, see Fig. 1. We look for stationary axisymmetric states with chemical potential μ and integer vorticity S as solutions to Eq. (1) in the form of

$$\Psi(\mathbf{r}, t) = \psi(r)\exp\left(iS\theta - i\mu t\right), \tag{4}$$

where θ is the angular coordinate. Self-trapped GS solutions are characterized by the total norm,

$$N = 2\pi\int_0^\infty \psi^2(r) r dr, \tag{5}$$

and the angular momentum, $M = SN$. Its energy is

$$E = E_{\rm K} + E_{\rm V} + E_{\rm DDI}, \tag{6}$$

where $E_{\rm K}$, $E_{\rm V}$ and $E_{\rm DDI}$ are the kinetic, potential, and DDI terms, respectively:

$$E_{\rm K} = \int |\nabla\psi|^2 d\mathbf{r} \equiv \pi\int_0^\infty \left[\left(\frac{d\psi}{dr}\right)^2 + \frac{S^2}{r^2}\psi^2(r)\right] r dr, \tag{7}$$

$$E_{\rm V} = 2\pi\int V(r)\psi^2(r) r dr, \tag{8}$$

$$E_{\rm DDI} = \frac{\kappa}{2}\iint R(\mathbf{r}-\mathbf{r}')|\psi(\mathbf{r})|^2|\psi(\mathbf{r}')|^2 d\mathbf{r} d\mathbf{r}'. \tag{9}$$

Two-dimensional bright GSs can be supported by the interplay of the radially periodic potential and repulsive interaction [64]. In this work, we focus on the DDI,

which was not previously considered in the present setting, neglecting contact interactions, which can be effectively suppressed by means of the Feshbach resonance [83]. In fact, effects of adding moderately strong contact interactions to the DDI were checked too (not shown in detail in this paper, as no dramatic changes in the results were observed in that case).

Numerical simulations have been carried out by dint of algorithm of PCSOM [82], fixing $\kappa \equiv 1$ by means of scaling, and, typically, taking $\epsilon = 0.5$, which is small enough in comparison with the potential's period, π, making it possible to produce generic results. It was additionally checked that taking still smaller ϵ (e.g., 0.25) does not produce any conspicuous change in the results. The stability of stationary soliton solutions was tested by means of real-time propagation, which was implemented with the help of the standard split-step – fast-Fourier-transform algorithm.

III. NUMERICAL RESULTS

A. The radial lattice with $\delta = 0$ (potential maximum at the center)

When radial potential (3), has a maximum at the center, Eq. (1), naturally, cannot produce a fundamental soliton ($S = 0$) with a density peak at $r = 0$. Instead, the model readily produces stable GSs with $S = 0, 1, 2, 3, 4, ...$ which feature a density minimum at the center, and the main radial density peak trapped in a trough with the bottom at one of potential minima,

$$r_{\min} = \pi \left(n - \frac{1}{2} \right), \ n = 1, 2, 3, 4, ..., \tag{10}$$

where n is the number of the radial minimum. Typical examples of such ring-shaped solitons are displayed in Fig. 2 for $S = 0$, and in Fig. 3 for $S = 1$ and $S = 4$. The GSs with $S = 0$ and 1 place their density maxima close to $n = 1$, while the vortex with $S = 4$ chooses $n = 3$. It is worthy to note than the latter vortex mode, with a high value of the topological charge, $S = 4$, displayed in Fig. 3(d-f), is definitely stable, on the contrary to a majority of models where it would be unstable. In fact, we have obtained stable vortex solitons with topological charges up to $S = 11$, as indicated below in Figs. 5(a) and 9(d).

Systematic numerical results, collected in Figs. 4 and 5(a), demonstrates that the GSs with $S = 0$ and 1 are trapped in the trough with $n = 1$, GSs with $S = 2$ and 3 choose $n = 2$, ones $S = 4$ and 5 choose $n = 3$, and so on, obeying an empiric relation

$$n_{\text{main peak}} = 1 + [S/2], \tag{11}$$

where [] stands for the integer part. Figure 5(a) also shows that the vortex modes with odd S have their energy decreasing with the growth of S, while the energy of ones with even S exhibit a very slow increase of the energy, starting from $S = 2$. Further, the mode with odd S has its energy always higher than its counterpart with even vorticity, $S - 1$, sharing the same position of the density maximum.

The linear dependence in Eq. (11) for large S can be explained in a qualitative form. Indeed, the strongest dependence of the energy of ring-shaped solitons on the ring's radius, $R \approx \pi n$ for large n [see Eq. (10)], is provided by the second term in Eq. (7), $E_S \approx (S/R)^2 N$ [for comparison, the DDI energy, defined as per Eq. (9), can be estimated as $\sim \kappa N^2/R$]. On the other hand, the energy term which provides for the trapping of the ring-shaped mode in the annular trap, is estimated as $E_{\text{trap}} \approx 2V_0 N$. Then , the balance of the two terms predicts $R \sim S/\sqrt{V_0}$.

The dependence of the chemical potential, μ, on norm N, which is displayed in Fig. 5(b) for the GS families with $S = 0, 1, 2, 3$, demonstrates that they obey the *anti-Vakhitov-Kolokolov criterion*, $\mathrm{d}\mu/\mathrm{d}N > 0$, which is a necessary condition for stability of solitons supported by any kind of repulsive nonlinearity [84, 85]. The same is true for still larger values of S, up to $S = 11$ (largest S considered in the present work).

B. The radial lattice with $\delta = \pi$ (potential minimum at the center)

1. *Fundamental gap solitons ($S = 0$)*

Radial potential (3) with $\delta = \pi$ gives rise to a set of potential minima

$$r_{\min} = \pi n, \ n = 0, 1, 2, 3, ..., \tag{12}$$

cf. Eq. (10). In this case, is natural to expect the existence of stable fundamental GSs with a density peak at $r = 0$, which corresponds to the zeroth minimum, in terms of Eq. (12). This expectation is borne out by numerical results, see a typical example in Fig. 6.

To characterize the family of the fundamental GSs, we define its effective area as

$$A_{\text{eff}} = \frac{\left(\int |\psi(x,y)|^2 \mathrm{d}x\mathrm{d}y \right)^2}{\int |\psi(x,y)|^4 \mathrm{d}x\mathrm{d}y}. \tag{13}$$

Along with the chemical potential, μ, it is shown, as a function of the norm, N, and the potential depth, V_0, in Fig. 7. In particular, Fig. 7(a,b) show that, quite naturally, the size of the fundamental GS increases when the self-repulsive DDI becomes stronger, but decreases with the growth of the trapping potential. Further, Fig. 7(c) corroborates that these solitons satisfy the anti-Vakhitov-Kolokolov criterion. In agreement with this finding, the family of the fundamental GSs is entirely stable.

Finally, the transition from $\mathrm{d}\mu/\mathrm{d}V_0 > 0$ in the relatively shallow radial lattice, at $V_0 < 2.3$, to $\mathrm{d}\mu/\mathrm{d}V_0 < 0$ at $V_0 > 2.3$ implies that properties of the soliton family

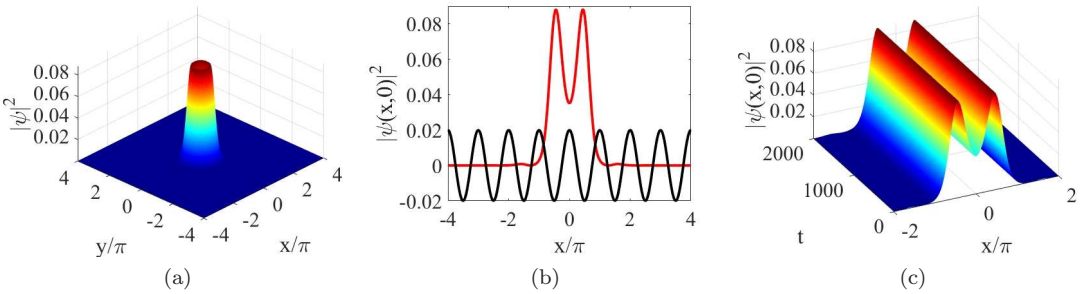

FIG. 2: (Color online) A typical fundamental ($S = 0, n = 1$) ring-shaped gap soliton for $\delta = 0$, other parameters being $N = 1.3$ and $V_0 = 1$. (a) The density of stationary wave function in the (x, y) plane. (b) Its cross section, $|\psi(x, 0)|^2$, along $y = 0$. (c) The cross-section of the real-time simulation, which demonstrates stability of the soliton.

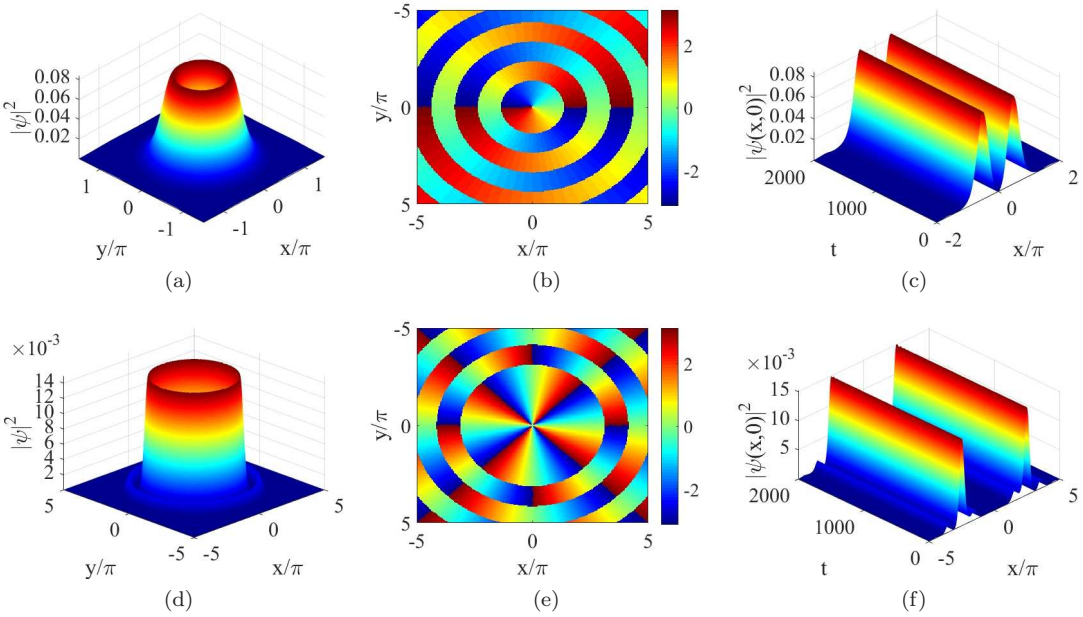

FIG. 3: (Color online) Two typical examples of stable gap-vortex solitons for $\delta = 0$. (a) and (b): Density and phase profiles of the vortex soliton for $S = 1, n = 1$ [n is defined as per Eq. (10)]. (c) The cross-section of the real-time evolution, corroborating the stability of the vortex soliton. (d,e,f) The same as in (a,b,c), respectively, but for $S = 4, n = 3$. The norm of both vortex solitons is $N = 1.3$, and the strength of the radial potential is $V_0 = 1$.

are dominated by the nonlinear interaction in the former case, and by the linear trapping potential in the latter one. Indeed, direct simulations demonstrate that the trapped mode with $S = 0$ "almost exists" in the deep potential with $V_0 > 2.3$ in the absence of the nonlinear interaction ($\kappa = 0$), exhibiting very slow decay.

2. *Ring-shaped and vortex solitons*

Besides the fundamental GSs trapped in the central potential well, the radial lattice with $\delta = \pi$ supports stable ring-shaped GSs, trapped in annular potential trough, also with $S = 0$, as well as ring-shaped vortex GSs. A typical example of the stable ring mode with $S = 0$, placed in the trough with $n = 1$, is displayed in Fig. 8. Further, Fig. 9 shows an example of a stable soliton with high vorticity, $S = 5$, which is trapped in the trough with $n = 3$ [see Eq. (12)].

Numerical results produce the same relation between the location of the ring-shaped solitons and their vorticity which is identified above for the radial potential with $\delta = 0$, see Eq. (11) (the same explanation for the linear dependence on large values of S, as that outlined above, is relevant in the present case too). Namely, the GSs with $S = 0$ and 1 are trapped in the trough with $n = 1$ in Eq. (12), ones with $S = 2$ and 3 are placed at $n = 2$, the solitons with $S = 4$ and 5 are trapped in the trough with $n = 3$, etc. These results are summarized in Fig. 9(d). Similar to the case of $\delta = 0$ [cf. Fig. 5(a)], the energy of the trapped states with odd S is higher than the energy of their counterparts with even vorticity, $S - 1$, with the

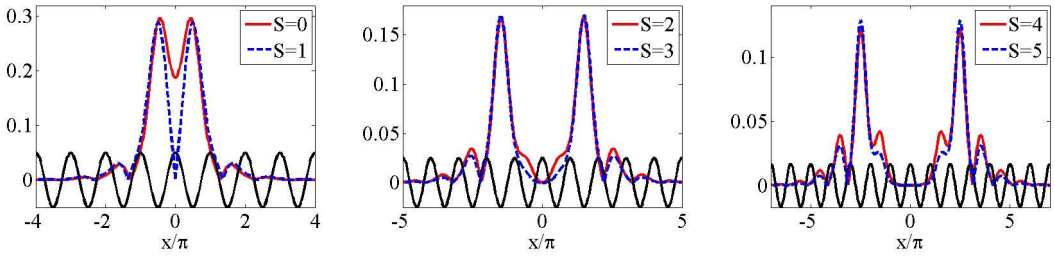

FIG. 4: (Color online) (a) The cross-section $|\psi(x,0)|$ of profiles of the gap solitons trapped in different annular potential troughs (here we display the absolute value of the field, rather than the density, to display the profiles in a clearer form). (a) The solitons with $S = 0$ and 1 in the first trough, which corresponds to $n = 1$ in Eq. (10). (b) $S = 2$ and 3, in the trough with $n = 2$. (c) $S = 4$ and 5, in the trough with $n = 3$. The norm of all the gap solitons displayed here is $N = 1.3$, and the half-depth of the periodic potential is $V_0 = 1$.

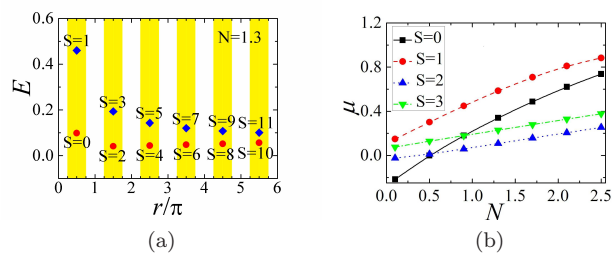

FIG. 5: (Color online) (a) The energy, defined by Eqs. (6)-(9), of the gap solitons with different vorticities S, and the radial location of their main density peaks. Yellow stripes denote the respective potential troughs. The norm of all the solitons presented in this panel is $N = 1.3$. (b) Chemical potential, μ, for the gap-soliton families with different values of S, versus the norm, N, at $V_0 = 1$. This panel demonstrates that all the families satisfy the anti- Vakhitov-Kolokolov criterion, $\mathrm{d}\mu/\mathrm{d}N > 0$, which is a necessary condition for the stability of solitons supported by a repusive nonlinearity (see the main text).

same position of the density maximum. A difference from the case of $\delta = 0$ is that the modes with even S feature increase of their energy with the growth of S, starting from $S = 2$, while the energy of the modes with odd S remain virtually constant.

C. Stable coexistence of double and multiple solitons

The existence of stable ring-shaped GSs with different topological charges, located in different annular potential troughs, suggests that such modes with different values of S may have a chance to coexist in the system as concentric modes, one embedded into the other. The coexistence of adjacent layers with different topological charges implies that they must be separated by zero-amplitude circular lines. Numerical results, produced by direct simulations of inputs built as superpositions of two ring vortices corroborate this conjecture, if the radial separation between the concentric rings is large enough (i.e., the interaction between them is sufficiently weak), as shown in Figs. 10(a-c). Due to the relation between the radial location of the ring soliton and S [as per Eq. (11)], the latter condition implies that the concentric rings must pertain to sufficiently different values of S. Moreover, Figs. 10(d,e) demonstrate a similar result produced by the initial superposition of three concentric GSs, under the same condition that they are separated well enough. On the other hand, an input with conspicuous overlap between the initial vortex rings gives rise to unstable evolution, see Fig. 10(f,g).

IV. CONCLUSION

We have elaborated a setting which makes it possible to readily stabilize bright vortex solitons with arbitrarily high values of the topological charge, S. The setting is realized as a two-dimensional dipolar BEC trapped in an axisymmetric radially periodic potential, with dipole moments of particles polarized perpendicular to the system's plane, which gives rise to the isotropic repulsive DDI (dipole-dipole interaction). The radial potentials with both the maximum and minimum at the center were considered. The interplay of the radial lattice potential and repulsive interactions creates families of stable annular GSs (gap solitons) with $S = 0$ and $S \geq 1$. Unlike the similar setting with contact repulsive interactions [64], where the annular vortex GSs are (weakly) unstable, the present system gives rise to GS families which are completely stable (at least, up to $S = 11$). The ring-shaped GSs have their main density peak located in an annular potential trough whose number grows, for large S, as $S/2$ [see Eq. (11)]. The linear growth of the vortex' radial location with S was qualitatively explained on the basis of the energy considerations. Further, sets of concentric annular GSs with sufficiently large radial separation between them, i.e., with essentially different values of S,

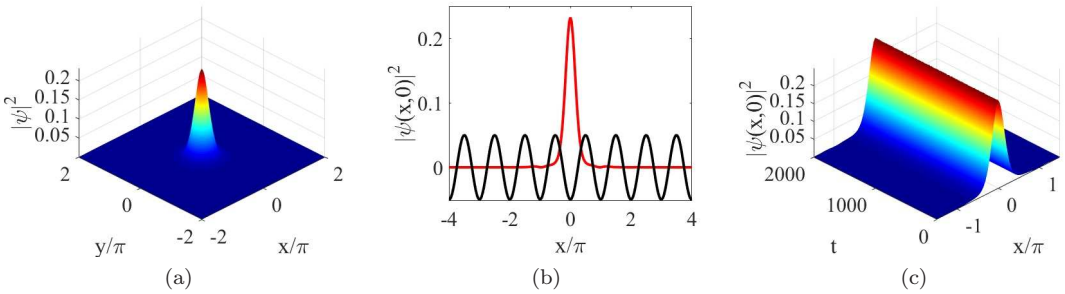

FIG. 6: (color online). A fundamental ($S = 0$) gap soliton trapped in the center of the radial lattice potential (3) with $\delta = \pi$. (a) The density profile of the soliton $|\psi(x, y)|^2$. (b) Its cross-section, $|\psi(x, 0)|^2$. (c) The cross-section of the simulated evolution of $|\psi(x, 0)|^2$, which demonstrates stability of the soliton. Its norm is $N = 0.5$, and the strength of the potential is $V_0 = 2$ in this case.

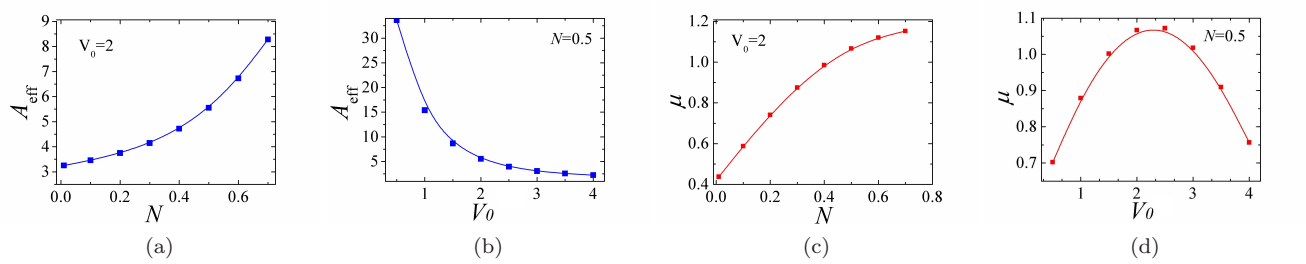

FIG. 7: (Color online) (a,b) A_{eff} for the fundamental gap soliton ($S = 0$), trapped in the central well of radial potential with $\delta = \pi$ [$n = 0$ in Eq. (12)], versus N and V_0, respectively. In panel (a) $V_0 = 2$, and in (b) $N = 0.5$. (c) μ versus N with $V_0 = 2$. (d) μ versus V_0 with $N = 0.5$. Other parameters are $\kappa = 1$ and $\epsilon = 0.5$.

stably coexist in the present system. The optical angular momentum becoming an important factor in modern information-processing technologies [86, 87], the setting analyzed in this work may find application to the storage of data encoded in values of the vorticity.

A challenging extension of the work is to construct three-dimensional bright GSs with embedded vorticity in the dipolar BEC, which will make it necessary to combine the radial potential with the a term which periodically varies along the transverse coordinate, z [such as $\cos(qz)$], so as to build an axially stacked version of the radial potential lattice, that should feature a full three-dimensional bandgap in its spectrum.

Acknowledgments

This work is supported by the National Natural Science Foundation of China (Grant Nos. 11575063, 11204037, 61575041). B.A.M. appreciates a Ding Ying visiting professorship provided by the South China Agricultural University (Guangzhou). The work of this authors is supported, in part, by the joint program in physics between NSF and Binational (US-Israel) Science Foundation through project No. 2015616, and by the Israel Science Foundation through grant No. 12876/17.

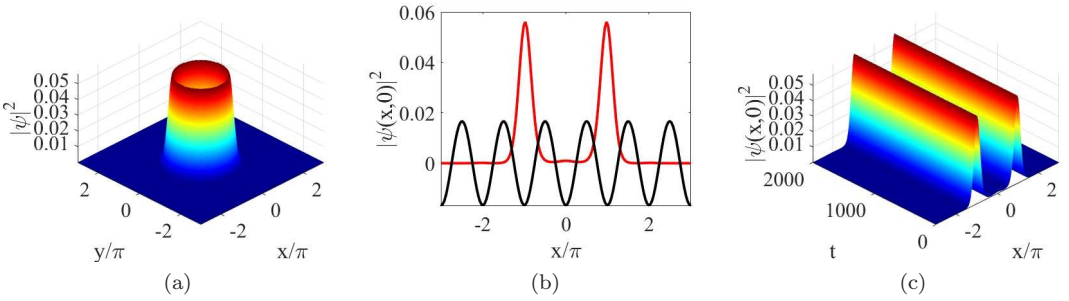

FIG. 8: (Color online) A typical example of the fundamental ring soliton ($S = 0$) trapped in the radial potential (3) with $\delta = \pi$. (a) The density profile of this gap soliton, $|\psi(x, y)|^2$. (b) Its cross-section, $|\psi(x, 0)|^2$, which clearly shows that it is trapped in the annular trough with $n = 1$, see Eq. (12). (c) Cross-section of the simulated evolution, which confirms the stability of the soliton. The norm of the soliton is $N = 1.3$, and the half-depth of the radial potential is $V_0 = 2$.

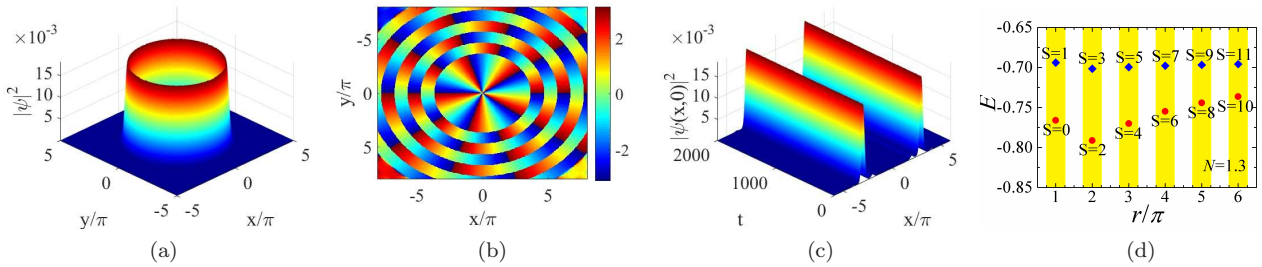

FIG. 9: (Color online) An example of a stable vortex gap soliton with a high topological charge, $S = 5$, trapped in the third annular trough of the radial potential (3) with $\delta = \pi$. Parameters are $N = 1.3$ and $V_0 = 2$. (a) and (b): The density and phase profiles of the vortex soliton. (c) The cross-section of the simultated evolution, which corroborates the stability of the vortex. (d) The same as in Fig. 5(a), but for potential (3) with $\delta = \pi$ (the energy of the soliton with $S = 0$ trapped at the center of the lattice, $n = 0$, is $E_0 = 1.943$, which is not displayed in this panel, as it is much larger than the values presented here). Other parameters are fixed as $N = 1.3$, $V_0 = 2$.

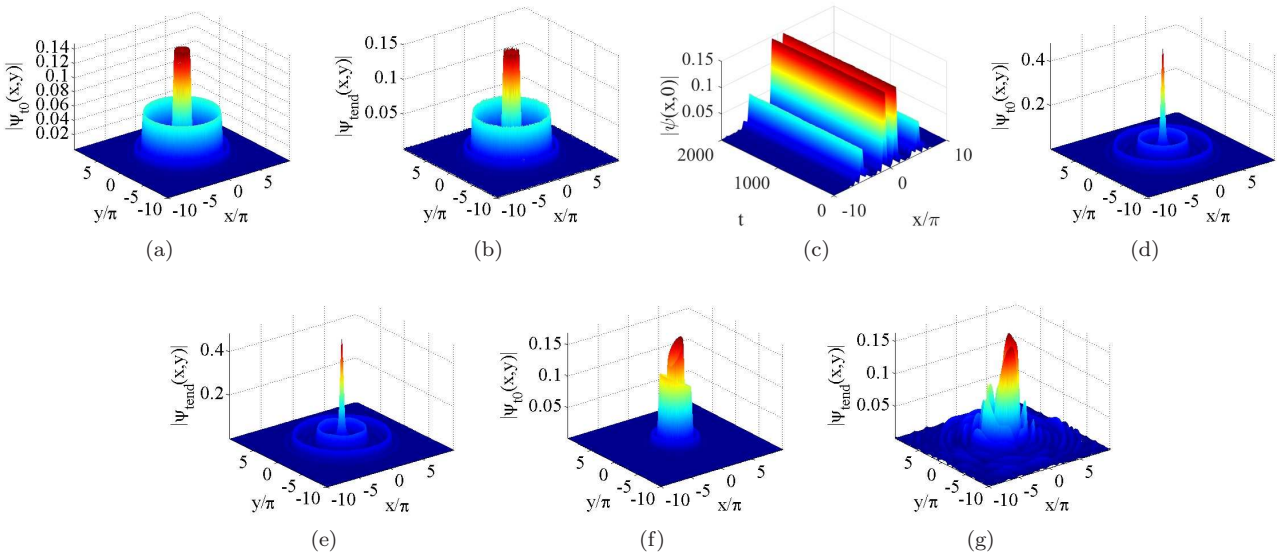

FIG. 10: (Color online) (a) The absolute-value profile of the concentric superposition of ring vortices with $S = 1$ and $S = 8$ (inner and outer rings, respectively), used as an input for direct simulations, with potential (3) that has a minimum at the center ($\delta = \pi$). (b) The output pattern of the simulation initiated by the input in (a) at $t = 2000$. (c) The cross-section along the x axis, illustrating the stable evolution of the concentric complex in the direct simulations. (d) The same as in (a), but with the input formed by the concentric superposition of three rings, with $S = 0$ (placed at the the center), $S = 4$, and $S = 10$. (e) The stable output pattern produced by the evolution of the input from (d) at $t = 2000$. (f) The same as in (a), but for the input taken as a superposition of ring vortices with $S = 1$ and $S = 2$; in this case, a conspicuous interference in observed in the input. (h) The result of unstable evolution initiated by the input from (f). In all the cases, parameters are $N = 0.5$ and $V_0 = 2$.

[1] P. Coullet, L. Gil, and F. Rocca, Optical vortices, Opt. Commun. **73**, 403 (1989).

[2] G. A. Swartzlander, Jr. and C. T. Law, Optical vortex solitons observed in Kerr nonlinear media, Phys. Rev. Lett. **69**, 2503 (1992).

[3] G. Duree, M. Morin, G. Salamo, M. Segev, B. Crosignani, P. D. Porto, E. Sharp, and A. Yariv, Dark Photorefractive Spatial Solitons and Photorefractive Vortex Solitons, Phys. Rev. Lett. **74**, 1978 (1995).

[4] A. S. Desyatnikov, Y. S. Kivshar, and L. Torner, Optical vortices and vortex solitons, Prog. Opt. **47**, 291-391 (2005).

[5] K. Kasamatsu, M. Tsubota, and M. Ueda, Vortices in multicomponent Bose-Einstein condensates, Int. J. Mod. Phys. B **19**, 1835-1904 (2005)

[6] R. Srinivasan, Vortices in Bose-Einstein condensates: A review of the experimental results, Pramana J. Phys. **66**, 3-130 (2006).

[7] S. Franke-Arnold, L. Allen, and M. Padgett, Advances in optical angular momentum, Laser & Photon. Rev. **2**, 299-313 (2008).

[8] M. R. Matthews, B. P. Anderson, P. C. Haljan, D. S. Hall, C. E. Wieman, and E. A. Cornell, Vortices in a Bose-Einstein condensate, Phys. Rev. Lett. **83**, 2498 (2009).

[9] A. L. Fetter, Rotating trapped Bose-Einstein condensates, Rev. Mod. Phys. **81**, 647-691 (2009).

[10] V. Achilleos, P. G. Kevrekidis, D. J. Frantzeskakis, and R. Carretero-González, Dark solitons and vortices in $\mathcal{PT}$-symmetric nonlinear media: From spontaneous symmetry breaking to nonlinear $\mathcal{PT}$ phase transitions, Phys. Rev. A **86**, 013808 (2012).

[11] C. L. Arnold, S. Akturk, A. Mysyrowicz, V. Jukna, A. Couairon, T. Itina, R. Stoian, C. Xie, J. M. Dudley, F. Courvoisier, S. Bonanomi, O. Jedrkiewicz and P. Di Trapani, Nonlinear Bessel vortex beams for applications, J. Phys. B: At. Mol. Opt. Phys. **48**, 094006 (2015).

[12] R. Barboza, U. Bortolozzo, M. G. Clerc, S. Residori, and E. Vidal-Henriquez, Optical vortex induction via light-matter interaction in liquid-crystal media, Adv. Opt. Phot. **7,** 635-683 (2015).

[13] M. Soskin, S. V. Boriskina, Y. Chong, M. R. Dennis, and A. Desyatnikov, Singular optics and topological photonics. J. Opt. **19**, 010401 (2017).

[14] F. Dalfovo and S. Stringari, Bosons in anisotropic traps: Ground state and vortices, Phys. Rev. A **53**, 2477-2485 (1996).

[15] M. Quiroga-Teixeiro and H. Michinel, Stable azimuthal stationary state in quintic nonlinear optical media, J. Opt. Soc. Am. B **14**, 2004-2009 (1997).

[16] V. I. Berezhiani, V. Skarka, and N. B. Aleksić, Dynamics of localized and nonlocalized optical vortex solitons in cubic-quintic nonlinear media, Phys. Rev. E **64**, 057601 (2001).

[17] R. L. Pego and H. A. Warchall, Spectrally Stable Encapsulated Vortices for Nonlinear Schrödinger Equations, J. Nonlin. Sci. **12**, 347-394 (2002).

[18] B. A. Malomed and P. G. Kevrekidis, Discrete vortex solitons, Phys. Rev. E, **64**, 026601 (2002).

[19] T. J. Alexander and L. Bergé, Phys. Rev. E **65**, Ground states and vortices of matter-wave condensates and optical guided waves, 026611 (2002).

[20] S. K. Adhikari, Mean-field model of interaction between bright vortex solitons in Bose-Einstein condensate, New J. Phys. **5**, 137 (2003).

[21] J. Yang, and D. E. Pelinovsky, Stable vortex and dipole vector solitons in a saturable nonlinear medium, Phys. Rev. E **67**, 016608 (2003).

[22] S. K. Adhikari, Stabilization of bright solitons and vortex solitons in a trapless three-dimensional Bose-Einstein condensate by temporal modulation of the scattering length, Phys. Rev. A **69**, 063613 (2004).

[23] D. Mihalache, D. Mazilu, B. A. Malomed, and F. Lederer, Stable vortex solitons supported by competing quadratic and cubic nonlinearities, Phys. Rev. E **69**, 066614 (2004).

[24] D. Mihalache, D. Mazilu, B. A. Malomed, and F. Lederer, Stable vortex solitons in a vectorial cubic-quintic model. J. Opt. B: Quant. Semicl. Opt. **6**, S341-S350 (2004).

[25] D. N. Neshev, T. J. Alexander, E. A. Ostrovskaya, Y. S. Kivshar, H. Martin, I. Makasyuk, and Z. Chen, Observation of discrete vortex solitons in optically induced photonic lattices, Phys. Rev. Lett. **92**, 123903 (2004).

[26] J. W. Fleischer, G. Bartal, O. Cohen, O. Manela, M. Segev, J. Hudock, and D. N. Christodoulides, Observation of vortex-ring "discrete" solitons in 2D photonic lattices, Phys. Rev. Lett. **92**, 123904 (2004).

[27] A. S. Desyatnikov, D. Mihalache, D. Mazilu, B. A. Malomed, C. Denz, and F. Lederer, Two-dimensional solitons with hidden and explicit vorticity in bimodal cubic-quintic media, Phys. Rev. E 71, 026615 (2005).

[28] A. I. Yakimenko, Y. A. Zaliznyak, and Y. Kivshar, Stable vortex solitons in nonlocal self-focusing nonlinear media, Phys. Rev. E **71**, 065603(R) (2005).

[29] C. Rotschild, O. Cohen, O. Manela, M. Segev, and T. Carmon, Solitons in nonlinear media with an infinite range of nonlocality: First observation of coherent elliptic solitons and of vortex-ring solitons, Phys. Rev. Lett. **95**, 213904 (2005).

[30] A. S. Desyatnikov, A. A. Sukhorukov, and Y. S. Kivshar, Azimuthons: Spatially modulated vortex solitons, Phys. Rev. Lett. **95**, 203904(2005).

[31] M. J. Paz-Alonso and H. Michinel, Superfluidlike motion of vortices in light condensates, Phys. Rev. Lett. **94**, 093901 (2005).

[32] L. D. Carr and Charles W. Clark, Vortices in attractive Bose-Einstein condensates in two dimensions, Phys. Rev. Lett. **97**, 010403 (2006).

[33] D. Mihalache, D. Mazilu, F. Lederer, Y. V. Kartashov, L.-C. Crasovan, L. Torner, and B. A. Malomed, Stable vortex tori in the three-dimensional cubic-quintic Ginzburg-Landau equation, Phys. Rev. Lett. **97**, 073904(2006).

[34] D. Mihalache, D. Mazilu, B. A. Malomed, and F. Lederer, Vortex stability in nearly-two-dimensional Bose-Einstein condensates with attraction, Phys. Rev. A **73**, 043615 (2006).

[35] Y. V. Kartashov, A. A. Egorov, V. A. Vysloukh, and L. Torner, Surface vortex solitons, Opt. Exp. **14**, 4049 (2006).

[36] A. A. Minzoni, N. F. Smyth, A. L. Worthy, and Y. S. Kivshar, Stabilization of vortex solitons in nonlocal nonlinear media, Phys. Rev. A **76**, 063803 (2007).

[37] J. Wang and J. Yang, Families of vortex solitons in peri-

odic media, Phys. Rev. A **77**, 033834 (2008).
[38] L. Dong, H. Wang, W. Zhou, X. Yang, X. Lv, and H. Chen, Necklace solitons and ring solitons in Bessel optical lattices, Opt. Exp. **16**, 5649 (2008).
[39] Y. J. He, B. A. Malomed, D. Mihalache, and H. Z. Wang, Crescent vortex solitons in strongly nonlocal nonlinear media, Phys. Rev. A **78**, 023824 (2008).
[40] W. Zhong and M. Belić, Three-dimensional optical vortex and necklace solitons in highly nonlocal nonlinear media, Phys. Rev. A **79**, 023804(2009).
[41] V. Skarka, N. B. Aleksić, H. Leblond, B. A. Malomed, and D. Mihalache, Varieties of Stable Vortical Solitons in Ginzburg-Landau Media with Radially Inhomogeneous Losses, Phys. Rev. Lett. **105**, 213901 (2010).
[42] Y. Wu, Q. Xie, H. Zhong, L. Wen, and W. Hai, Algebraic bright and vortex solitons in self-defocusing media with spatially inhomogeneous nonlinearity, Phys. Rev. A **87**, 055801 (2013).
[43] M. Shen, H. Zhao, B. Li, J. Shi, Q. Wang, and R. Lee, Stabilization of vortex solitons by combining competing cubic-quintic nonlinearities with a finite degree of nonlocality, Phys. Rev. A **89**, 025804 (2014).
[44] Z. Chen, J. Liu, S. Fu, Y. Li, and B. A. Malomed, Discrete solitons and vortices on two-dimensional lattices of $\mathcal{PT}$-symmetric couplers, Opt. Exp. **22**, 29679 (2014).
[45] Y. V. Kartashov, B. A. Malomed, Y. Shnir, and L. Torner, Twisted toroidal vortex solitons in inhomogeneous media with repulsive nonlinearity, Phys. Rev. Lett.. **113**, 264101 (2014).
[46] R. Driben, Y. V. Kartashov, B. A Malomed, T. Meier, and L. Torner, Three-dimensional hybrid vortex solitons, New J. Phys. **16** 063035 (2014).
[47] N. Dror and B. A. Malomed, Solitons and vortices in nonlinear potential wells, J. Optics **16**, 014003 (2016)
[48] J. Qin, G. Dong, and B. A. Malomed, Stable giant vortex annuli in microwave-coupled atomic condensates, Phys. Rev. A **94**, 053611 (2016).
[49] B. Liao, S. Li, C. Huang, Z. Luo, W. Pang, H. Tan, B. A. Malomed, and Y. Li, Anisotropic semivortices in dipolar spinor condensates controlled by Zeeman splitting, Phys. Rev. A **96**, 043613 (2017).
[50] H. Sakaguchi, B. Li, B. A. Malomed, Creation of two-dimensional composite solitons in spin-orbit-coupled self-attractive Bose-Einstein condensates in free space, Phys. Rev. E **89**, 032920 (2014).
[51] Y. Zhang, Z. Zhou, B. A. Malomed, and H. Pu, Stable Solitons in Three Dimensional Free Space without the Ground State: Self-Trapped Bose-Einstein Condensates with Spin-Orbit Coupling, Phys. Rev. Lett. **115**, 253902 (2015).
[52] X. Jiang, Z. Fan, Z. Chen, W. Pang, Y. Li, and B. A. Malomed, Two-dimensional solitons in dipolar Bose-Einstein condensates with spin-orbit coupling, **93**, 023633 (2016).
[53] H. Sakaguchi, E. Y. Sherman, and B. A. Malomed, Vortex solitons in two-dimensional spin-orbit coupled Bose-Einstein condensates: Effects of the Rashba-Dresselhaus coupling and Zeeman splitting, Phys. Rev. E **90** 032202(2016).
[54] S. Gautam and S. K. Adhikari, Vortex-bright solitons in a spin-orbit-coupled spin-1 condensate, Phys. Rev. A **95**, 013608 (2017).
[55] G. Chen, Y. Liu, and H. Wang, Mixed-mode solitons in quadrupolar BECs with spin-orbit coupling, Commun. Nonlinear Sci. Numer. Simulat. **48**, 318 (2017).
[56] Y. Li, Y. Liu, Z. Fan, W. Pang, S. Fu, and B. A. Malomed, Two-dimensional dipolar gap solitons in free space with spin-orbit coupling, Phys. Rev. A, **95**, 063613 (2017).
[57] J. M. Soto-Crespo, D. R. Heatley, E. M. Wright, and N. N. Akhmediev, Stability of the higher-bound states in a saturable self-focusing medium, Phys. Rev. A **44**, 636 (1991).
[58] D. V. Skryabin and W. J. Firth, Dynamics of self-trapped beams with phase dislocation in saturable Kerr and quadratic nonlinear media, Phys. Rev. E **58**, 3916 (1998).
[59] M. Soljačíc, S. Sears, and M. Segev, Self-Trapping of Necklace Beams in Self-Focusing Kerr Media, Phys. Rev. Lett. **81**, 4851 (1998).
[60] A. S. Desyatnikov and Y. S. Kivshar, Necklace-Ring Vector Solitons, Phys. Rev. Lett. **87**, 033901 (2001).
[61] M. Soljačíc and M. Segev, Integer and Fractional Angular Momentum Borne on Self-Trapped Necklace-Ring Beams, Phys. Rev. Lett. **86**, 420 (2001).
[62] D. V. Petrov, L. Torner, J. Martorell, R. Vilaseca, J. P. Torres, and C. Cojocaru, Observation of azimuthal modulational instability and formation of patterns of optical solitons in a quadratic nonlinear crystal, Opt. Lett. **23**, 1444-1446 (1998).
[63] Y. V. Kartashov, V. A. Vysloukh, and L. Torner, Stable Ring-Profile Vortex Solitons in Bessel Optical Lattices, Phys. Rev. Lett. **94**, 043902 (2005).
[64] B. B. Baizakov, Boris A. Malomed, and Mario Salerno, Matter-wave solitons in radially periodic potentials. Phys. Rev. E **74**, 066615 (2006).
[65] S. Sinha and L. Santos, Cold dipolar gases in quasi-one-dimensional geometries, Phys. Rev. Lett. **99**, 140406 (2007).
[66] J. Cuevas, B. A. Malomed, P. G. Kevrekidis, and D. J. Frantzeskakis, Solitons in quasi-one-dimensional Bose-Einstein condensates with competing dipolar and local interactions, Phys. Rev. A **79**, 053608 (2009).
[67] F. Kh. Abdullaev, A. Gammal, B. A. Malomed, and L. Tomio, Bright solitons in quasi-one dimensional dipolar condensates with spatially modulated interactions, Phys. Rev. A **87**, 063621 (2013).
[68] T. Bland, M. J. Edmonds, N. P. Proukakis, A. M. Martin, D. H. J. O'Dell, and N. G. Parker, Controllable nonlocal interactions between dark solitons in dipolar condensates, Phys. Rev. A **92**, 063601 (2015).
[69] P. Pedri and L. Santos, Two-Dimensional Bright Solitons in Dipolar Bose-Einstein Condensates, Phys. Rev. Lett. **95**, 200404 (2005).
[70] I. Tikhonenkov, B. A. Malomed, and A. Vardi. Anisotropic solitons in dipolar Bose-Einstein condensates. Phys. Rev. Lett. **100**, 090406 (2008).
[71] I. Tikhonenkov, B. A. Malomed, and A. Vardi, Vortex solitons in dipolar Bose-Einstein condensates, Phys. Rev. A **78**, 043614 (2008).
[72] G. Gligorić, A. Maluckov, M. Stepić, L. Hadžievski, and B. A. Malomed, Two-dimensional discrete solitons in dipolar Bose-Einstein condensates, Phys. Rev. A **81**, 013633 (2010).
[73] G. Gligorić, A. Maluckov, L. Hadžievski, and B. A. Malomed, Discrete vortex solitons in dipolar Bose-Einstein condensates, J. Phys. B **43**, 055303 (2010).
[74] P. Köberle, D. Zajec, G. Wunner, and B. A. Malomed, Creating two-dimensional bright solitons in dipolar Bose-

Einstein condensates, Phys. Rev. A **85**, 023630 (2012).
[75] Y. Li, J. Liu, W. Pang, and B. A. Malomed, Matter-wave solitons supported by field-induced dipole-dipole repulsion with spatially modulated strength, Phys. Rev. A **88**, 053630 (2013).
[76] M. Raghunandan, C. Mishra, K. Lakomy, P. Pedri, L. Santos, and R. Nath, Two-dimensional bright solitons in dipolar Bose Einstein condensates with tilted dipoles, Phys. Rev. A **92**, 013637 (2015); X. Chen, Y. Chuang, C. Lin, C. Wu, Y. Li, B. A. Malomed, R. Lee, A magic tilt angle for stabilizing two-dimensional solitons by dipole-dipole interactions, arXiv:1709.01646 (2017).
[77] Y. Xu, Y. Zhang, and C. Zhang, Bright solitons in a two-dimensional spin-orbit-coupled dipolar Bose-Einstein condensate, Phys. Rev. A **92**, 013633 (2015).
[78] H. Chen, Y. Liu, Q. Zhang, Y. Shi, W. Pang, and Y. Li, Dipolar matter-wave solitons in two-dimensional anisotropic discrete lattices, Phys. Rev. A **93**, 053608 (2016).
[79] P. Muruganandam and S. K. Adhikari, Gap solitons in a dipolar Bose-Einstein condensate on a three-dimensional optical lattice. J. Phys. B: At. Mol. Opt. Phys. **44**, 121001(2011).
[80] Y. Li, J. Liu, W. Pang, and B. A. Malomed, Lattice solitons with quadrupolar intersite interactions, Phys. Rev. A **88**, 063635 (2013).
[81] J. Huang, X. Jiang, H. Chen, Z. Fan, W. Pang, and Y. Li, Quadrupolar matter-wave soliton in two-dimensional free space, Front. Phys. **10**, 100507 (2015).
[82] J. Yang and T. I. Lakoba. Universally-convergent squared-operator iteration methods for solitary waves in general nonlinear wave equations. Stud. Appl. Math. **118**, 153-197 (2007).
[83] C. Chin, R. Grimm, P. Julienne, and E. Tiesinga, Feshbach resonances in ultracold gases, Rev. Mod. Phys. **82**, 1225-1286 (2010).
[84] M. Vakhitov and A. Kolokolov, Stationary solutions of the wave equation in a medium with nonlinearity saturation,Radiophys. Quantum Electron. **16**, 783 (1973).
[85] H. Sakaguchi and B. A. Malomed, Solitons in combined linear and nonlinear lattice potentials, Phys. Rev. A **81**, 013624 (2010).
[86] J. Wang, J. Y. Yang, I. M. Fazal, N. Ahmed, Y. Yan, H. Huang, Y. X. Ren, Y. Yue, S. Dolinar, M. Tur, and A. E. Willner, Terabit free-space data transmission employing orbital angular momentum multiplexing, Nature Phot. **6**, 488-496 (2012).
[87] N. Bozinovic, Y. Yue, Y. X. Ren, M. Tur, P. Kristensen, H. Huang, A. E. Willner, S. Ramachandran, Terabit-scale orbital angular momentum mode division multiplexing in fibers, Science **340**, 1454-1548 (2013).